Journal of Physics: Conference Series **1526** (2020) 012004 doi:10.1088/1742-6596/1526/1/012004

# First observation and study of the $K^{\pm} \to \pi^{\pm}\pi^0 e^+ e^-$ decay with the NA48/2 experiment at CERN

**B Bloch-Devaux**[1,2]

[1] Università di Torino, Dipartimento di Fisica Sperimentale, Torino, Italy

E-mail: brigitte.bloch-devaux@cern.ch

**Abstract.** The first observation of the rare decay $K^{\pm} \to \pi^{\pm}\pi^0 e^+ e^-$ is reported by the NA48/2 experiment at CERN, based on 4919 candidates with 4.9% background contamination. From the analysis of $1.7 \times 10^{11}$ kaon decays collected in 2003–2004, the branching ratio in the full kinematic region is measured to be BR($K^{\pm} \to \pi^{\pm}\pi^0 e^+ e^-$)= $(4.24 \pm 0.14) \times 10^{-6}$. A detailed study of the kinematic space shows evidence for a structure dependent contribution. Both measured BR and structure dependent contribution are in perfect agreement with theoretical predictions based on Chiral Perturbation Theory. Several P- and CP-violating asymmetries are also evaluated.

## 1. Introduction

Kaon decays have played a major role in establishing the quark mixing flavour structure of the Standard Model. Radiative kaon decays, dominated by long-distance effects, are particularly suited in testing models describing low-energy quantum chromodynamics (QCD) such as the chiral perturbation theory (ChPT), an effective field theory valid below a scale of $\mathcal{O}(1$ GeV). The $K^{\pm} \to \pi^{\pm}\pi^0 e^+ e^-$decay, never observed so far, proceeds through virtual photon exchange followed by internal conversion into an electron-positron pair, i.e. $K^{\pm} \to \pi^{\pm}\pi^0\gamma^* \to \pi^{\pm}\pi^0 e^+ e^-$.

The virtual $\gamma^*$ can be produced by two different mechanisms: Inner Bremsstrahlung (IB), where the $\gamma^*$ is emitted by one of the charged mesons in the initial or final state and Direct Emission (DE) where the $\gamma^*$ is radiated off at the weak vertex. Consequently, the differential

[2] for the NA48/2 Collaboration: G. Anzivino, R. Arcidiacono, W. Baldini, S. Balev, J.R. Batley, M. Behler, S. Bifani, C. Biino, A. Bizzeti, B. Bloch-Devaux, G. Bocquet, N. Cabibbo, M. Calvetti, N. Cartiglia, A. Ceccucci, P. Cenci, C. Cerri, C. Cheshkov, J.B. Chèze, M. Clemencic, G. Collazuol, F. Costantini, A. Cotta Ramusino, D. Coward, D. Cundy, A. Dabrowski, P. Dalpiaz, C. Damiani, M. De Beer, J. Derré, H. Dibon, L. DiLella, N. Doble, K. Eppard, V. Falaleev, R. Fantechi, M. Fidecaro, L. Fiorini, M. Fiorini, T. Fonseca Martin, P.L. Frabetti, L. Gatignon, E. Gersabeck, A. Gianoli, S. Giudici, A. Gonidec, E. Goudzovski, S. Goy Lopez, M. Holder, P. Hristov, E. Iacopini, E. Imbergamo, M. Jeitler, G. Kalmus, V. Kekelidze, K. Kleinknecht, V. Kozhuharov, W. Kubischta, G. Lamanna, C. Lazzeroni, M. Lenti, L. Litov, D. Madigozhin, A. Maier, I. Mannelli, F. Marchetto, G. Marel, M. Markytan, P. Marouelli, M. Martini, L. Masetti, E. Mazzucato, A. Michetti, I. Mikulec, M. Misheva, N. Molokanova, E. Monnier, U. Moosbrugger, C. Morales Morales, D.J. Munday, A. Nappi, G. Neuhofer, A. Norton, M. Patel, M. Pepe, A. Peters, F. Petrucci, M.C. Petrucci, B. Peyaud, M. Piccini, G. Pierazzini, I. Polenkevich, Yu. Potrebenikov, M. Raggi, B. Renk, P. Rubin, G. Ruggiero, M. Savrié, M. Scarpa, M. Shieh, M.W. Slater, M. Sozzi, S. Stoynev, E. Swallow, M. Szleper, M. Valdata-Nappi, B. Vallage, M. Velasco, M. Veltri, S. Venditti, M. Wache, H. Wahl, A. Walker, R. Wanke, L. Widhalm, A. Winhart, R. Winston, M.D. Wood, S.A. Wotton, A. Zinchenko, M. Ziolkowski.

decay rate consists of three terms: the dominant long-distance IB contribution (electric part E only), the DE component (both electric E and magnetic M parts), and their interference. The interference term collects the different contributions, IB-E, IB-M and E-M. The P-violating IB-M and E-M terms cancel upon angular integration and do not contribute to the total rate. Few theoretical publications investigate the $K^{\pm} \to \pi^{\pm}\pi^0 e^+ e^-$mode [1][2][3] and no experimental observation has so far been reported. The authors of [2] were able to predict, on the basis of the NA48/2 measurement of the magnetic and electric terms in the $K^{\pm} \to \pi^{\pm}\pi^0\gamma$ decay mode [4], the contributions of the single components relative to IB. Including more experimental measurements from radiative kaon decays [5], the authors of [3] were able to refine their predictions.

## 2. The NA48/2 experiment

The NA48/2 experiment at the CERN SPS was specifically designed for charge asymmetry measurements in the $K^{\pm} \to 3\pi$ decay modes [6] and collected large samples of charged kaon decays during the 2003–2004 data taking period. The experiment beam line had been designed to deliver simultaneous narrow momentum band $K^+$ and $K^-$ beams originating from primary 400 GeV/$c$ protons extracted from the CERN SPS and impinging on a beryllium target. Secondary unseparated beams with central momenta of 60 GeV/$c$ and a momentum band of $\pm 3.8\%$ (rms) were selected and brought to a common beam axis. A fraction of the beam kaons decayed in a fiducial decay volume contained in a 114 m long cylindrical evacuated tank. The momenta of charged decay products were measured in a magnetic spectrometer, housed in a tank filled with helium and placed downstream of the decay volume. The spectrometer was composed of four drift chambers (DCH) and a dipole magnet providing in the horizontal plane a momentum kick $\Delta p = 120$ MeV/$c$ to charged particles. The momentum resolution achieved was $\sigma_p/p = (1.02 \oplus 0.044 \cdot p)\%$ ($p$ in GeV/$c$). A hodoscope (HOD) consisting of two planes of plastic scintillators, each segmented into 64 strip-shaped counters, followed the spectrometer and provided time measurements for charged particles with a resolution of 150 ps. The HOD surface was logically subdivided into 16 exclusive regions producing fast signals used to trigger the detector readout on charged track topologies. Further downstream was a liquid krypton electromagnetic calorimeter (LKr), an almost homogeneous ionization chamber with an active volume of 7 m$^3$ of liquid krypton, $27X_0$ deep, segmented transversally into 13248 projective $\sim$2$\times$2 cm$^2$ cells and with no longitudinal segmentation. The energies of photons were measured with a resolution $\sigma_E/E = (3.2/\sqrt{E} \oplus 9.0/E \oplus 0.42)\%$ ($E$ in GeV). An iron/scintillator hadronic calorimeter and muon detectors, not used in the present analysis, were located further downstream. A dedicated two-level trigger was used to collect three track decays with a very high efficiency [6]. A detailed description of the detector can be found in [7].

## 3. Analysis strategy and measurements

Events in the signal mode are selected simultaneously with events in the normalization mode ($K^{\pm} \to \pi^{\pm}\pi^0_D, \pi^0_D \to \gamma e^+ e^-$) chosen to have a final state topology ($\pi^{\pm}\gamma e^+ e^-$) differing from the signal ($\pi^{\pm}\gamma\gamma e^+ e^-$) by only one photon while satisfying similar kinematic constraints on the reconstructed $\pi^0$ and kaon masses.

### *3.1. Candidate selections and background estimates*

Both signal and normalization candidates are reconstructed from three charged tracks (two same-sign tracks and one opposite-charge track) forming a common vertex in the fiducial decay volume. The tracks are required to be in time within 5 ns of each other using the HOD time of the hit associated to the track and their impact point should lie within the geometrical acceptance of the drift chambers (radial distance to the beam line axis, monitored by fully reconstructed $K^{\pm} \to \pi^{\pm}\pi^+\pi^-(K_{3\pi})$ events, larger than 12 cm). The track momenta are required to be in the range (2–60) GeV/$c$ and any track-to-track distance at DCH1 should be larger than 2 cm to

suppress photon conversions to an $e^+e^-$ pair in the upstream material. The first level trigger requires coincidences of hits in the two HOD planes in at least two of the 16 square regions. Events with all three tracks hitting the same HOD quadrant, leading to geometrical inefficiency, are rejected to ensure high and similar trigger efficiencies for both modes.

Isolated energy clusters without associated track in the LKr, in time within 5 ns with the mean of the three track times, are identified as the photon candidates. The minimum photon energy required is 2 GeV. The photon four-momenta are reconstructed assuming they originate from the 3-track vertex.

In the signal selection, the two-photon invariant mass is required to be within $\pm 15$ MeV/$c^2$ from the nominal PDG [8] $\pi^0$ mass. The reconstructed invariant mass of the $\pi^\pm\pi^0e^+e^-$system is required to be within $\pm 45$ MeV/$c^2$ from the nominal PDG $K^\pm$ mass. In the normalization selection, the same cuts applies to the invariant mass of the $\gamma e^+e^-$ system ($\pi^0_D$) and to the $\pi^\pm\pi^0_D$ system, respectively. The strong kinematic correlation between the reconstructed $\pi^0$ and kaon masses is exploited, selecting events in a band defined as $|m_{\pi^0} - 0.42 \times m_K + 73.2| < 6$ MeV/$c^2$ (masses in MeV/$c^2$), allowing particle identification without using the LKr information for electron-pion separation. More than 99% of the normalization simulated events and 96.5% of the signal simulated events satisfy the requirement.

The total reconstructed momentum is required to be in the range (54–66) GeV/$c$, compatible with the beam momentum. In the transverse plane, the reconstructed 3-track vertex position and kaon position at the LKr front face (defined as the energy weighted sum of the non-deviated tracks and photon(s) positions) are required to be consistent with the corresponding beam positions as monitored by $K_{3\pi}$ events.

Two main sources of background are contributing to the signal final state: $K^\pm \to \pi^\pm\pi^0\pi^0_D$ ($K_{3\pi D}$) when one of the photons is lost, and $K^\pm \to \pi^\pm\pi^0_D(\gamma)$ ($K_{2\pi D}$), when an extra photon combines with the Dalitz photon to mimic a $\pi^0 \to \gamma\gamma$ decay. An additional suppression of the $K_{3\pi D}$ background events is obtained by requiring the squared invariant mass of the $\pi^+\pi^0$ system to be greater than 0.12 GeV$^2/c^4$, exploiting the larger phase space available in the signal mode. To reject further $K_{2\pi D}$ background contamination, each of the two possible invariant masses $M_{ee\gamma}$ are required to be more than 7 MeV/$c^2$ away from the nominal mass of the neutral pion. The background processes contributing to the normalization mode are $K_{\mu 3D}(K^\pm \to \mu^\pm\nu\pi^0_D)$ and $K_{e3D}$ ($K^\pm \to e^\pm\nu\pi^0_D$) where the $\pi^0_D$ is correctly reconstructed but the muon (electron) is given a pion mass and therefore can sometimes satisfy all other selection criteria.

Samples of $16.3 \times 10^6 K_{2\pi D}$ and 4919 signal candidates have been selected from a subset of a $1.7 \times 10^{11}$ kaon decay exposure in 2003–2004. The background contributions are estimated from simulation. They amount to $(10437 \pm 119)$ $K_{\mu 3D}$ events and $(6851 \pm 106)$ $K_{e3D}$ events in the normalization mode, corresponding to a total background contamination of $(0.106 \pm 0.001)\%$. In the signal mode, they amount to $(132 \pm 8)$ events from $K_{3\pi D}$, $(102 \pm 19)$ events from $K_{2\pi D}$ and $(7 \pm 3)$ events from $K_{e3D}$, adding up to a relative background contribution of $(4.9 \pm 0.4)\%$. Reconstructed mass distributions are displayed in Figure 1 (Figure 2) for the selected normalization (signal) candidates. Expected background and normalization (signal) simulations, scaled to the number of observed candidates, show a good agreement with the data distributions.

*3.2. Branching ratio measurement*

The Branching Ratio of the $K^\pm \to \pi^\pm\pi^0e^+e^-$decay mode is obtained using the expression:

$$\mathrm{BR}(K^\pm \to \pi^\pm\pi^0e^+e^-)/\mathrm{BR}(K^\pm \to \pi^\pm\pi^0) = \frac{(N_s - N_{bs})}{(N_n - N_{bn})} \cdot \frac{A_n \times \varepsilon_n}{A_s \times \varepsilon_s} \cdot \frac{\Gamma(\pi^0_D)}{\Gamma(\pi^0_{\gamma\gamma})} \qquad (1)$$

where $N_{s,bs,n,bn}$ are the number of signal, background to signal, normalization and corresponding background events. $A_{s,n}$ and $\varepsilon_{s,n}$ are the acceptances and trigger efficiencies of the signal and

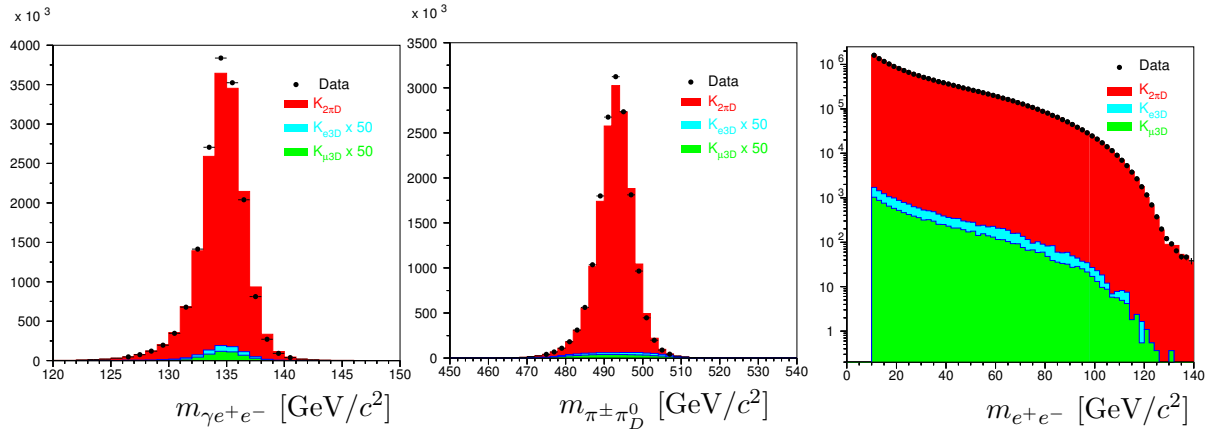


**Figure 1.** Normalization candidates. Left: reconstructed $\gamma e^+e^-$ mass. Middle: reconstructed $\pi^\pm\pi^0_D$ mass. Right: reconstructed $e^+e^-$ mass. The selection requires $m_{e^+e^-} > 10$ MeV/$c^2$. Dots correspond to data candidates, stacked histograms are, from bottom to top, the expected $K_{\mu 3D}$ (green) and $K_{e3D}$ (blue) backgrounds multiplied by a factor of 50 to be visible. The normalization simulation (red) includes radiative effects.

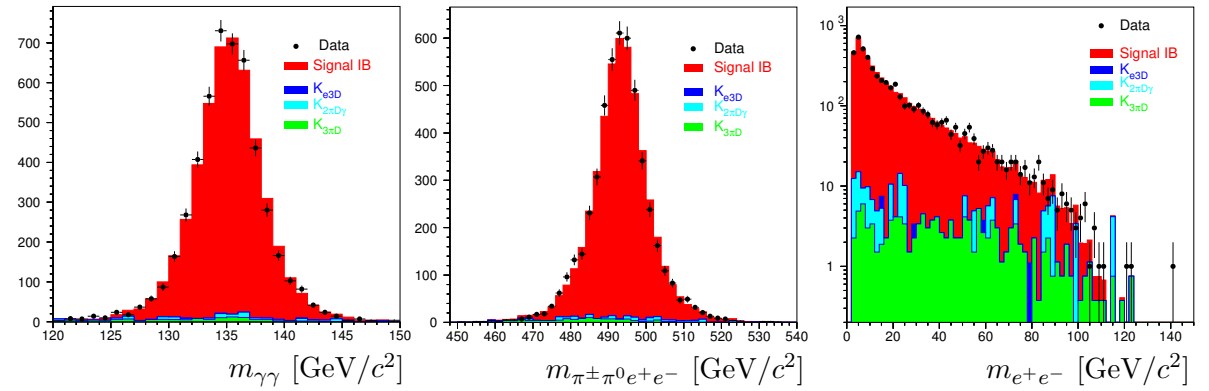


**Figure 2.** Signal candidates. Left: reconstructed $\gamma\gamma$ mass. Middle: reconstructed $\pi^\pm\pi^0e^+e^-$ mass. Right: reconstructed $e^+e^-$ mass. Full dots correspond to data candidates, stacked histograms are, from bottom to top, the expected $K_{3\pi D}$ (green), $K_{2\pi D}$ (light blue) and $K_{e3D}$ (dark blue) backgrounds and signal IB (red) estimated from simulation.

normalization modes. The trigger efficiency ($\varepsilon_n$), is measured using control data samples. It is also evaluated on simulated samples and found to be well reproduced ($\varepsilon_n = 98.27(1)\%$). Because of the very limited data statistics, simulated signal samples are therefore used to evaluate the signal trigger efficiency ($\varepsilon_s = 98.34(2)\%$) . The normalization mode branching ratio BR($K^\pm \to \pi^\pm\pi^0$) $= (20.67 \pm 0.08) \times 10^{-2}$ is obtained from the PDG [8] world average. The acceptances of the signal, the normalization and the background channels are computed using a GEANT3-based [9] Monte Carlo (MC) simulation which includes full detector geometry and material description, stray magnetic fields, accurate beam line geometry, local detector imperfections and time variations of the above throughout the data taking period. The $A_n$ acceptance of 3.981(2)% is computed using the implementation of $K^\pm \to \pi^\pm\pi^0$ according to [10] followed by $\pi^0_D$ according to the most recent calculations [11], including the best current

implementation of radiative effects. The agreement between data and simulation can be seen from the $m_{e^+e^-}$ distribution of Figure 1. The MC simulations for the different $\pi^\pm\pi^0e^+e^-$ contributions IB, DE, and the electric interference IB-E, have been generated separately according to the theoretical description given in [2][3] neglecting the magnetic interference. The $A_s$ acceptance of 0.662(1)% has been obtained from a weighted average of the single component acceptances, using as weights the relative contributions with respect to IB computed in [2][3]. As radiative corrections to the $\pi^\pm\pi^0e^+e^-$ mode are not considered in [2][3], the signal MC simulation included the real photon(s) emission as implemented in the PHOTOS package. The total branching ratio is obtained as :

$$\mathrm{BR}(K^\pm \to \pi^\pm\pi^0e^+e^-) = (4.237 \pm 0.063_{stat} \pm 0.033_{syst} \pm 0.126_{ext}) \times 10^{-6} \quad (2)$$

where systematic errors include uncertainties on acceptance, trigger efficiencies and radiative corrections. The external error originating from the $\pi^0_D$ branching ratio uncertainty is the dominant error in the present measurement obtained with an overall precision of 2.971%.

*3.3. Kinematic space study and asymmetries*

The obtained BR measurement is in very good agreement with the theoretical predictions [2][3] of $4.18 \times 10^{-6}$ for IB only and $4.23 \times 10^{-6}$ including all structure dependent contributions but is not precise enough to distinguish between them. Within the current statistics, the data sample analyzed has no sensitivity to the DE and INT contributions that would be dominant in the upper part of the $m_{ee}$ spectrum (Figure 2). However a global analysis of the 3d-space $(q^2, T^*_\pi, E^*_\gamma)$ where $q^2, T^*_\pi, E^*_\gamma$ are the $e^+e^-$ mass squared, the charged pion kinetic energy and the virtual photon energy in the kaon rest frame, respectively, allows to measure the fractions M/IB $= (1.14 \pm 0.43_{stat})$%, to be compared to the prediction $(1.41 \pm 0.14_{ext})$% and, with a limited accuracy, (IB-E)/IB $= (-0.14 \pm 0.36_{stat})$%, to be compared to the prediction $(-0.39 \pm 0.28_{ext})$%. The external errors stem from the uncertainties of the measurements used as input in the predictions.

Asymmetries between $K^+$ and $K^-$ partial rates give access to the weak (or beyond Standard Model) phases that change sign under charge conjugation, unlike the strong phase that governs the final state interaction of the pion system. The simplest CP-violating asymmetry is the charge asymmetry of the integrated partial rates, $A_{CP}$, measured from the statistically independent measurements of $K^+$ and $K^-$ branching ratios, as $A_{CP} = (-2.84 \pm 1.55)$%, translated to a single-sided upper limit of $|A_{CP}| < 4.82$% at 90% CL. Similarly, other asymmetries can be built from partially integrated $K^+$ and $K^-$ partial rates over the angular variable $\phi$, the angle between the dipion and dilepton planes in the kaon rest frame. Two CP-violating asymmetries and one long-distance P-violating asymmetry [5] have been evaluated, all consistent with zero and resulting in single-sided upper limits $|A^\phi_{CP}| < 1.9$% at 90% CL and $|A^{(L)}_P| < 1.8$% at 90% CL .

## 4. Summary

The first observation of the $K^\pm \to \pi^\pm\pi^0e^+e^-$decay has been reported by the NA48/2 collaboration [12] with a branching ratio $\mathrm{BR}(K^\pm \to \pi^\pm\pi^0e^+e^-) = (4.24 \pm 0.14) \times 10^{-6}$ in agreement with the theoretical predictions [2][3]. The relative contribution M/IB has been evaluated from a 3d-analysis of the kinematic space as $(1.14 \pm 0.43_{stat})$%. Several P- and CP-violating asymmetries have been set as single-sided upper limits of ∼2% at 90% CL. Further studies of this rich mode could bring more information on the internal structure of the decay process, in a later data taking period of NA62 including a dedicated trigger stream.

## Acknowledgments
The author is most grateful to the local organisers of the KAON 2019 conference for making this contribution possible and for their support and hospitality.

## References
[1] Pichl H 2001 *Eur. Phys. J.* C **20** 371
[2] Cappiello L, Catà O, D'Ambrosio G and Gao D N 2012 *Eur. Phys. J.* C **72** 1872
[3] Cappiello L, Catà O and D'Ambrosio G 2018 *Eur. Phys. J.* C **78** 265
[4] Batley J R *et al.* [NA48/2 Collaboration] 2010 *Eur. Phys. J.* C **68** 75
[5] Catà O, 2019 these proceedings
[6] Batley J R *et al.* [NA48/2 Collaboration] 2007 *Eur. Phys. J.* C **52** 875
[7] Fanti V *et al.* 2007 *Nucl. Instrum. Methods* A **574** 443
[8] Tanabashi M *et al.* [Particle Data Group] 2018 *Phys. Rev.* D **98** 030001
[9] GEANT3 Detector Description and Simulation Tool 1994 *CERN Program Library* W**5013**
[10] Gatti C 2006 *Eur. Phys. J.* C **45** 417
[11] Husek T, Kampf K and Novotny J 2015 *Phys. Rev.* D **92** 054027
[12] Batley J R *et al.* [NA48/2 Collaboration] 2019 *Phys. Lett.* B **788** 552